Plant Science 203–204 (2013) 79–88

Contents lists available at SciVerse ScienceDirect

Plant Science

journal homepage: www.elsevier.com/locate/plantsci

Molecular properties of the class III subfamily of acyl-coenyzme A binding proteins from tung tree (*Vernicia fordii*)

Steven Pastor[a,1], Kandan Sethumadhavan[a], Abul H.J. Ullah[a], Satinder Gidda[b], Heping Cao[a], Catherine Mason[a], Dorselyn Chapital[a], Brian Scheffler[c], Robert Mullen[b], John Dyer[d], Jay Shockey[a,*]

[a] Southern Regional Research Center, United States Department of Agriculture-Agricultural Research Service, 1100 Robert E. Lee Blvd., New Orleans, LA 70124, USA
[b] Department of Molecular and Cellular Biology, Room 4470 Science Complex, 488 Gordon Street, University of Guelph, Guelph, Ontario N1G 2W1, Canada
[c] USDA-ARS, MidSouth Area Genomics Laboratory, 141 Experiment Station Rd., Stoneville, MS 38776, USA
[d] USDA-ARS, U.S. Arid-Land Agricultural Research Center, 21881 North Cardon Lane, Maricopa, AZ 85138, USA

ARTICLE INFO

Article history:
Received 27 September 2012
Received in revised form
14 December 2012
Accepted 20 December 2012
Available online 9 January 2013

Keywords:
Acyl-CoA binding protein
Acyl-CoA binding domain
Phosphatidylcholine
Eleostearic acid
Triacylglycerol
Tung tree

ABSTRACT

Acyl-CoA binding proteins (ACBPs) have been identified in most branches of life, and play various roles in lipid metabolism, among other functions. Plants contain multiple classes of ACBP genes. The most diverse group is the class III proteins. Tung tree (*Vernicia fordii*) contains two such genes, designated *VfACBP3A* and *VfACBP3B*. The two proteins are significantly different in length and sequence. Analysis of tung *ACBP3* genes revealed significant evolution, suggesting relatively ancient divergence of the two genes from a common ancestor. Phylogenetic comparisons of multiple plant class III proteins suggest that this group is the most evolutionarily dynamic class of ACBP. Both tung *ACBP3* genes are expressed at similar levels in most tissues tested, but *ACBP3A* is stronger in leaves. Three-dimensional modeling predictions confirmed the presence of the conserved four α-helix bundle acyl-CoA binding (ACB); however, other regions of these proteins likely fold much differently. Acyl-CoA binding assays revealed different affinities for different acyl-CoAs, possibly contradicting the redundancy of function suggested by the gene expression studies. Subcellular targeting of transiently-expressed plant ACBP3 proteins contradicted earlier studies, and suggested that at least some class III ACBPs may be predominantly targeted to endoplasmic reticulum membranes, with little or no targeting to the apoplast.

Published by Elsevier Ireland Ltd.

1. Introduction

Fatty acids are an integral part of many biochemical pathways in plant cells. Few biological reactions utilize free fatty acids; most rely on activated precursors such as acyl-CoA. The thioester bond of acyl-CoA molecules is a high energy bond and is susceptible to cleavage by thioesterase enzymes and other hydrolases. Acyl-CoAs are also amphipathic and can have negative effects on membrane bilayer structure and stability [1]. Therefore, it is assumed that acyl-CoAs rarely exist in free form, but instead are complexed with acyl-CoA binding proteins (ACBP) in most living systems.

The prototype ACBP is a small protein, approximately 10 kDa in size. First described in yeast, ACBP is required for protein sorting, vesicular trafficking, sphingolipid synthesis, and fatty acid chain elongation in this organism [2,3]. Groundbreaking NMR spectroscopy and X-ray crystallography studies using the L-ACBP form of the protein from *Bos taurus* and *Plasmodium falciparum* revealed that L-ACBP forms an up-down-down-up four α-helix bundle protein. Essentially the entire length of the protein is contained within these four helices, which mainly interact through hydrophobic interactions to form a shallow non-polar bowl-like structure bounded by a highly polar rim [4–6].

This class of protein is ancestral and highly conserved [7]; basic homology searches using either the human or yeast protein readily detect orthologs from essentially every eukaryotic organism, including plants, for which genomic or transcriptomic data are available. Potential roles for this form of ACBP in plants (commonly called ACBP6 in this context) have arisen from various recent studies. *In vitro* studies with ACBP6 from oilseed rape (*Brassica napus*) suggest a role in the maintenance of

Abbreviations: ACBP, acyl-CoA binding protein; ACB, acyl-CoA binding domain; TAG, triacylglycerol; PC, phosphatidylcholine; PA, phosphatidic acid; SDS-PAGE, sodium dodecyl sulfate polyacrylamide gel electrophoresis; ER, endoplasmic reticulum; qPCR, real-time quantitative polymerase chain reaction; DGAT, diacylglycerol acyltransferase; GPAT, glycerol-3-phosphate acyltransferase.

* Corresponding author. Tel.: +1 504 286 4296; fax: +1 504 286 4367.
E-mail addresses: Jay.Shockey@ars.usda.gov, shockeyj@bellsouth.net (J. Shockey).
[1] Current address: Louisiana State University School of Medicine, 1901 Perdido Street, New Orleans, LA 70112, USA.

0168-9452/$ – see front matter. Published by Elsevier Ireland Ltd.
http://dx.doi.org/10.1016/j.plantsci.2012.12.009

equilibrium between metabolically active acyl-CoA and phospholipid pools necessary for proper fatty acid desaturation and triacylglycerol (TAG) synthesis [8]. ACBP6 is also a major protein of the phloem sap in several plants, including *B. napus*, coconut (*Cocos nucifera*), and multiple curcurbits, indicating a possible role in long distance acyl-CoA mediated signaling [9,10]. *Arabidopsis* ACBP6 enhances freezing tolerance [11], likely by altering the metabolism and/or intracellular transport of the phospholipid phosphatidylcholine (PC) thus altering the ratio of PC to phosphatidic acid (PA).

In some organisms however, multiple other classes of ACBP have evolved. In particular, studies in simple aquatic and higher land plants show that most plant species contain between 3 and 11 *ACBP* genes (including *ACBP6*), distributed across five distinct classes (designated classes I–IV and class 0) [12]. Many of these proteins are much larger than ACBP6 and have acquired other functional motifs in addition to the four α-helix bundle ACB domain. Not surprisingly, these proteins have also been implicated in a diverse array of cellular processes. Most of this work has been conducted using *Arabidopsis thaliana* in the laboratory of Mee-Len Chye, so the description of representative genes from each class will primarily focus on this species. *ACBP6* is the sole member of class I. Class II contains AtACBP1 and AtACBP2, two closely related enzymes that are localized to the ER and plasma membranes [13,14]. *Arabidopsis* overexpressing lines showed enhanced tolerance to heavy metals, suggesting that AtACBP1 and AtACBP2 may assist in phospholipid membrane repair following heavy metal stress [15,16]. Class II ACBPs also contain C-terminal ankyrin repeats. The functions of these proteins are at least partially redundant, but are essential for embryo development; *acbp1acbp2* double mutant lines are embryo lethal [17]. Class IV consists of AtACBP4 and AtACBP5. Both of these large cytosolic proteins contain kelch motifs and preferentially bind oleoyl-CoA esters. The class IV proteins may be good candidates for the long-known role of acyl-CoA export from the chloroplasts [18,19]. The presence of ankyrin repeats and kelch motifs, respectively, have helped to identify protein interactors of the class II and class IV proteins [15,20–22]. Class 0 ACBPs are found only in green algae, mosses and gymnosperms [12] and will not be discussed in detail here.

Class III ACBPs are particularly interesting. Unlike all other classes of ACBPs, which contain their ACB domains at or near their respective N-termini, all Class III proteins described to date [12,23] contain C-terminal ACB domains. Preliminary subcellular analysis of transiently expressed AtACBP3 lacking the ACB domain revealed targeting to the apoplast [23]. In-depth analysis of transgenic *Arabidopsis* plants expressing fusions of full length AtACBP3 to green fluorescent protein (GFP) revealed a more complex pattern of subcellular distribution, including intracellular membranes, the ER/Golgi complex, and the extracellular space. This targeting pattern was fully dependent on the presence of a transmembrane domain near the extreme N-terminus [24]. In addition to binding acyl-CoAs, AtACBP3 binds PC, and phosphatidylethanolamine (PE) *in vitro*. These properties help to explain the observation that AtACBP3 regulates leaf senescence by modulating phospholipid metabolism [24].

In our quest to identify enzymes and other important proteins that contribute to TAG biosynthesis in oilseeds, we identified four *ACBP* genes from developing seeds of tung tree. This list includes *VfACBP6*, representing class I, and *VfACBP4*, from class IV. Interestingly, two class III genes, *VfACBP3A* and *VfACBP3B* were also identified. The presence of two class III ACBPs in a given species is somewhat unusual, and led us to explore the similarities and differences in the properties of these two genes. These results are described in this report.

2. Materials and methods

2.1. EST analysis, gene identification and cloning

The tung seed cDNA library used for EST analysis was constructed previously [25] using the TriplEx system available from Clontech (Mountain View, CA, USA). This phage-based library was converted to a plasmid-based library by *cre-lox* mediated excision using *E. coli* strain BM25.8, as described by the manufacturer (Clontech). Single bacterial colonies were picked using an automated robotics system, followed by plasmid DNA isolation and DNA sequencing using plasmid-specific primers and dye terminated cycle sequencing and an Applied Biosystems Model 377 sequencer (Applied Biosystems, Foster City, CA, USA). Additional genes were discovered through analysis of assembled cDNA contig sequences and singletons generated through massively parallel ("454") pyrosequencing [26] of cDNA samples isolated from mid-development tung seeds collected during the 2006 growing season. Shelled seeds were frozen in liquid nitrogen and stored at −80 °C until use. Total RNA was isolated as described previously [27]. mRNA was isolated using the Ambion PolyA Purist MAG kit from Life Technologies (Carlsbad, CA, USA). cDNA was synthesized using the Clontech SMART PCR cDNA synthesis method. cDNA amplification by long distance-PCR was performed using Clontech Advantage2 PCR protocol (50 °C/27 cycles). The amplified cDNA was purified using Zymo Research DNA Clean & Concentrate kit (Irvine, CA, USA) and one portion was reserved as the non-normalized sample for 454 sequencing. The remainder of the purified cDNA was normalized using the protocol from the Evrogen (Moscow, Russia) Trimmer-Direct kit. This system involves a duplex specific nuclease (crab claw nuclease) to degrade the abundant transcripts, followed by PCR amplification of the normalized ssDNA fraction. Normalized and non-normalized samples were submitted for 454 sample prep and analysis at the USDA-ARS, MidSouth Area Genomics Laboratory (Stoneville, MS). Identified sequences were used to generate gene-specific primers that allowed for PCR amplification of both cDNA and genomic copies of the tung ACBP genes. Restriction sites present in the primers were used for restriction endonuclease digestion and cloning into vectors for sequencing, *E. coli* expression, and transient expression in onion epidermal cells and tobacco Bright Yellow-2 (BY-2) cell suspension cultures. The nucleotide sequence for tung acyl-CoA binding protein 6 (VfACBP6) cDNA was deposited in Genbank™ under accession number JX866759. The accession numbers for the other tung ACBPs are: JX866760 (VfACBP4 cDNA), JX866761 (VfACBP3A cDNA), JX866762 (VfACBP3A genomic), JX866763 (VfACBP3B cDNA), and JX866764 (VfACBP3B genomic).

2.2. Recombinant ACBP3 protein expression and purification

Portions of the ACBP3 proteins from tung and *Arabidopsis*, lacking the predicted N-terminal transmembrane helix domains, were cloned as N-terminal polyhistidine fusions by ligation of *Sac*II-*Not*I digested PCR products into the same sites of pET47b (EMD Millipore, Billerica, MA, USA), to generate plasmids pP20, pP30, and pP38. P20 contained the portion from E106 to the C-terminus of VfACBP3A, while P30 contained the region beginning with D150 of VfACBP3B. P38 expresses the region of AtACBP3 from Q162 to the C-terminus. These three plasmids were transformed into *E. coli* BL21(DE3) CodonPlus-RIPL competent cells (Agilent Technologies, Santa Clara, CA, USA) and colonies selected on solid LB agar medium containing kanamycin and chloramphenicol. Protein was produced and purified as described previously [28], with minor modifications. Single colonies with the plasmids were inoculated into 2X YT medium (16 g bactotryptone, 10 g yeast extract, 5 g NaCl per liter, pH 7.0, containing 50 μg/ml each kanamycin

and chloramphenicol), and grown overnight with shaking at 30 °C. The overnight cultures were inoculated at a 1:20 dilution into fresh medium and grown for about 4 h at 30 °C to reach an optical cell density of approximately 0.6–1.0 at OD_{600nm}. Isopropylthio-β-D-galactoside (IPTG) was added to the culture medium (0.5 mM final concentration) and protein expression was induced at 30 °C overnight. Cells were collected by centrifugation at 5000 × *g* for 10 min and homogenized by sonication in homogenization buffer (3 ml/g wet cells) containing nickel-nitrilotriacetic agarose (Ni-NTA agarose from Qiagen) resin wash buffer minus detergents (20 mM imidazole, 50 mM NaH_2PO_4, pH 7.4, 300 mM NaCl, 10 mM β-mercaptoethanol), plus 0.2 mM phenylmethylsulfonyl fluoride (PMSF), and 1:500 dilution of protease inhibitor cocktail (Sigma, cat #P8340). The homogenate was centrifuged at 2000 × *g* for 10 min to remove cell debris and the resulting supernatant was centrifuged at 10,000 × *g* for 15 min.

The recombinant ACBP3 was purified from *E. coli* by batch method from the 10,000 × *g* supernatant using Ni-NTA beads according to similar procedures [28]. The 10,000 × *g* supernatant was mixed with Ni-NTA Agarose (Qiagen). The mixtures were incubated at 4 °C with rotation overnight followed by packing the beads in a Bio-Rad mini-column. The beads were washed five times each with five bead-volumes of Ni-NTA resin wash buffer. The bound proteins were eluted from the beads by gravity flow with increasing concentrations of imidazole in Ni-NTA wash buffer. Each fraction was analyzed by SDS-PAGE. Fractions containing significant quantities of the target proteins were pooled, dialyzed against 10 mM potassium phosphate, pH 7.4, and concentrated. The final pooled products were evaluated for purity of the ACBP3 proteins by SDS-PAGE, and used for acyl-CoA binding assays.

2.3. Transient expression and subcellular targeting analysis

Tobacco (*Nicotiana tabacum* L. cv BY-2) suspension cell cultures were maintained and prepared for biolistic bombardment as described previously [29]. Transient transformations were performed using 5 μg of plasmid DNA with a biolistic particle delivery system (Bio-Rad Laboratories Ltd., Mississauga, Canada). Following bombardment, cells were incubated for 4–6 h to allow for expression and sorting of the introduced gene product(s). ConA conjugated to Alexa 594 (Molecular Probes, Eugene, OR, USA) was added to cells at a final concentration of 5 mg/ml for 20 min prior to imaging. Epifluorescent images of cells were acquired using an Axioscope 2 MOT epifluorescence microscope (Carl Zeiss, Toronto, Canada) with a 63X Plan Apochromat oil-immersion objective. Images were captured using a Retiga 1300 CCD camera (Qimaging, Burnaby, Canada) and Improvision Openlab software, and figures were composed using Adobe Photoshop CS (Adobe Systems, Ottawa, Canada). All micrographs shown are representative images obtained from at least two replicate biolistic experiments.

2.4. Quantitative Real-time Polymerase Chain Reaction (qPCR)

Real-time PCR was performed with a BioRad C1000 core unit PCR thermocycler with a BioRad CFX96 head unit for qPCR. The PCR reaction was carried out in a final volume of 25 μl, which included 2 μl cDNA, 10 μl Biorad SYBR Green master mix, 2.5 μl of 5 μM sense and antisense primers, and H_2O. The PCR conditions consisted of 40 cycles at 95 °C for 10 s, 60 °C for 10 s, and 72 °C for 30 s. The reference gene included with each run was tung ubiquitin ligase. Samples were assayed in triplicate; means and standard deviations were calculated from the data obtained. The data was normalized using BioRad software (BioRad CFX Manager version 1.5). Each baseline was adjusted based upon a value calculated by taking the baseline average of all the combined runs per gene.

2.5. Lipidex-1000™ acyl-CoA binding assay

Binding of semi-purified His6-fusion ACBP proteins to radiolabeled acyl-CoAs was performed using the Lipidex-1000™ binding assay (Packard BioScience, Groningen, the Netherlands), as previously described in [8] with minor modifications. Briefly, 3000 pmol of ACBPs were incubated with [^{14}C] oleoyl-CoA or [^{14}C] arachidonyl-CoA (0.1–2 μM) in 100 μl of binding buffer (10 mM potassium phosphate, pH 7.4) at 30 °C for 30 min. The mixture was then placed on ice for 10 min, and 100 μl of ice-cold 50% Lipidex-1000 slurry in binding buffer (v/v) were added. Samples were incubated on ice with occasional mixing for 20 min, and then centrifuged at 12,000 × *g* for 5 min at 4 °C. One hundred μl of the supernatant from each sample were combined with 5 ml of Ecolite scintillant (MP Biochemicals, Irvine, CA, USA) and analyzed for radioactivity in a scintillation counter (Beckman Coulter, LS-6500, Mississauga, ON, Canada). Control samples with no protein added were used to correct for the amount of acyl-CoA that was not absorbed by Lipidex-1000 beads.

2.6. ACBP three-dimensional protein structure prediction

The three-dimensional structures of ACBP proteins were predicted by Robetta, a full-chain protein structure prediction server, operated from Dr. David Baker's laboratory at the University of Washington (http://robetta.bakerlab.org/) [30]. The pdb files generated by the Robetta server were downloaded to local computers for further analysis. The structures were manipulated and visualized using both Deep-View/Swiss-Pdb Viewer (http://www.expasy.org/spdbv) and Chimera software (http://www.cgl.ucsf.edu/chimera/) [31]. Each structure was truncated using Deep-View, which produced new pdf files for each molecule.

2.7. Expression of tung ACBP3 in transgenic Arabidopsis thaliana

The open reading frames for tung FADX and tung ACBP3A were cloned into shuttle vectors containing the strong seed-specific promoters from the α′-subunit of soybean β-conglycinin [32] and *Arabidopsis thaliana 2S-4* albumin [33], respectively. The expression cassettes containing these genes were transferred to a binary vector containing a basta resistance gene, enabling selection of transgenic plants expressing resistance to herbicides containing glufosinate ammonium. *Arabidopsis thaliana* plants (*fad3fae1* mutant [34]) were transformed with constructs containing either tung FADX alone, or tung *FADX* plus tung *ACBP3A*. T_1 plants were selected on soil wetted with Finale® herbicide (Bayer CropScience, Research Triangle Park, North Carolina) and seeds were collected at maturity. Segregating T_2 seed pools were analyzed for α-eleostearic acid content by gas chromatography as described previously [27].

3. Results

3.1. Identification and comparison of tung ACBP cDNA clones

Two libraries of tung seed cDNA sequences were generated and analyzed: one expressed sequence tag collection consisting of approximately 5000 plasmid-based clones sequenced using traditional Sanger dideoxy chain terminator technology, and a second double-stranded cDNA sample subjected to 454 sequencing. Both datasets were compared to other existing databases using BLAST alignments and annotated to indicate their closest hits.

A full-length clone for a class I gene (designated *VfACBP6*) and a partial clone for a representative from class IV (*VfACBP4*) were identified. The remaining 5′ portion of *VfACBP4* was identified by

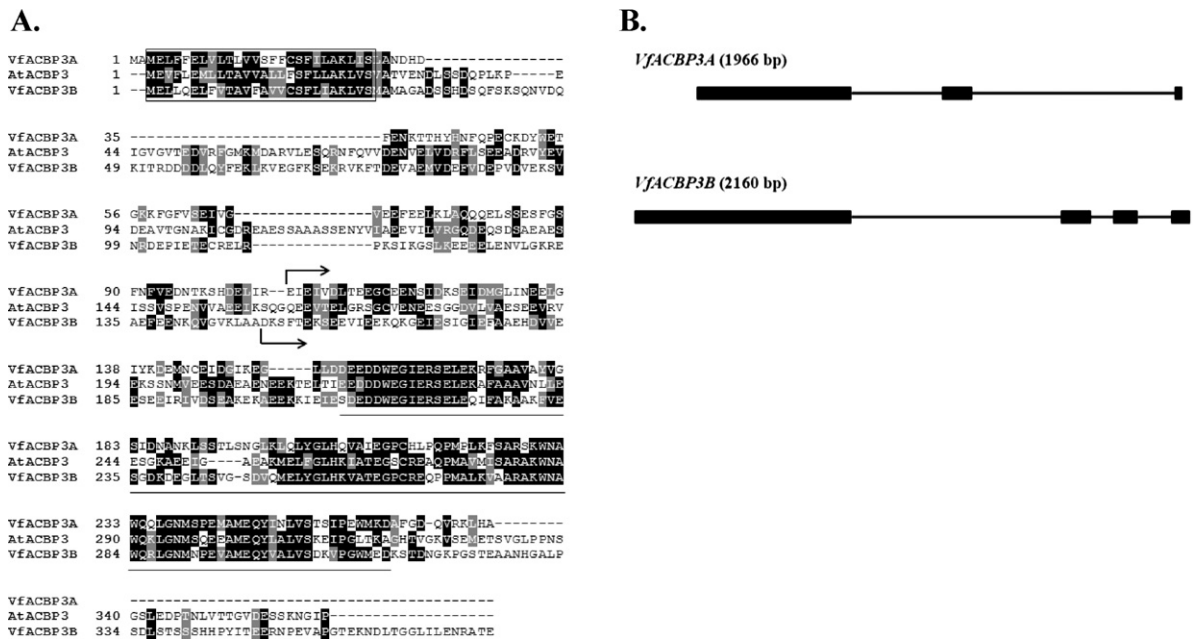

Fig. 1. (**A**) Alignment of predicted ACBP3 protein sequences of tung and *Arabidopsis*. The N-terminal transmembrane helical domain/signal transit peptide region (as predicted by TMHMM server, version 2.0, http://www.cbs.dtu.dk/services/TMHMM/) is boxed and the acyl-CoA binding domain is underlined. The first residues included in the polyhistidine fusion protein plasmid constructs are indicated by an over arrow for VfACBP3A E106 and AtACBP3 Q162, and an under arrow for VfACBP3B D150. The alignment was generated using ClustalX version 2.0.12 [45], and shaded using Boxshade version 3.21 (http://www.ch.embnet.org/software/BOX_form.html). (**B**) Genomic architecture of ACBP3 genes from tung. Exons are shown as boxes, and introns are shown as lines. All exons and introns are drawn to scale.

5′ RACE. VfACBP4 and VfACBP6 are both very strongly conserved amongst various plant species; the two proteins share 88% and 93% amino acid identity with their closest homologs in castor bean (*Ricinus communis*) and black cottonwood tree (*Populus trichocharpa*), respectively (data not shown). Full-length cDNA sequences for two additional candidate *ACBP* genes were also identified. Both most closely resembled AtACBP3 (and other plant class III *ACBP* genes), and were thus named *VfACBP3A* and *VfACBP3B*. Unlike the other orthologous tung genes, these two ACBPs were much more weakly conserved. Homology between the two proteins was restricted to the predicted C-terminal acyl-CoA binding domains, and to a much lesser extent, to the extreme N-termini, corresponding to a putative transmembrane domain (predicted by TMHMM server, version 2.0, http://www.cbs.dtu.dk/services/TMHMM/). VfACBP3B also contains a much longer extension C-terminal to the ACB domain relative to VfACBP3A. VfACBP3A and VfACBP3B share only 39% and 54% identity to their closest orthologous relatives from soybean (*Glycine max*) and castor bean, respectively. The central portion of the proteins were highly variable, with little conservation between the two tung ACBP3s, or between any pairings of the tung proteins to their orthologs from other plant species. A graphical representation of the alignment of the two tung proteins and AtACBP3 is shown in Fig. 1**A**.

3.2. Isolation and comparison of tung ACBP3 genomic clones

Gene duplication events are quite common in plants. Genes that have undergone relatively recent duplication can often be expected to retain similar exon/intron patterns, whereas genes generated through more ancient duplication events often evolve significantly different structures. The full-length genomic sequences for *tung ACBP3A* and *3B* were isolated to examine for similarities or differences in genomic architecture (Fig. 1B). The lengths of the first exons for both genes are similar, and the position of the splice site between the first exon and first intron in both genes is conserved. Otherwise the exon/intron patterns for these two genes are significantly different. *VfACBP3B* has four exons, compared to three for *VfACBP3A*, and the lengths and distribution of introns are not conserved between the two genes.

3.3. Phylogenetic analysis of different plant ACBP classes

The highly variable nature of the class III ACBPs can be also be visualized by comparing the degree of interspecies divergence between representative *ACBP* genes from each of the four main classes from multiple plant species. Using the BLAST function, at the Phytozome version 8.0 site (http://www.phytozome.net/, United States Department of Energy Joint Genome Institute and University of California Berkeley Center for Integrative Genomics), protein sequences designated ACBP2, ACBP3, ACBP4, and ACBP6 (representing classes II–IV, and I, respectively) were identified in the annotated proteomes of castor bean, *Arabidopsis*, and grape (*Vitus vinifera*). These sequences were aligned with and compared to the classes I–III ACBP proteins from tung. Fig. 2 contains a phylogenetic tree showing the relative degree of divergence between each of the plant ACBP proteins. With the lone exception of the divergent second class IV protein from grape (VvACBP4B), it is clear that the ACBP6 and ACBP4 subgroups are highly conserved across various orders of the plant kingdom. Class II proteins (ACBP2s) are somewhat less conserved. The ACBP3 proteins on the other hand all have significantly longer branch lengths, and hence, much lower levels of amino acid identity.

3.4. Tung ACBP3 gene expression profiling

The gene expression profiles for both tung class III ACBP genes were examined to search for insights into potential functions. Relatively little is known about the biological roles of this class. Previous studies of AtACBP3 indicate roles in phospholipid metabolism, pathogen defense, autophagy and leaf senescence [24,35]; the rice homolog (called OsACBP5, [12]) is the only other plant ACBP3-type protein described in the literature. RNA expression levels in flowers, young leaves, and developing seeds were determined by qPCR, and normalized expression levels for both genes are

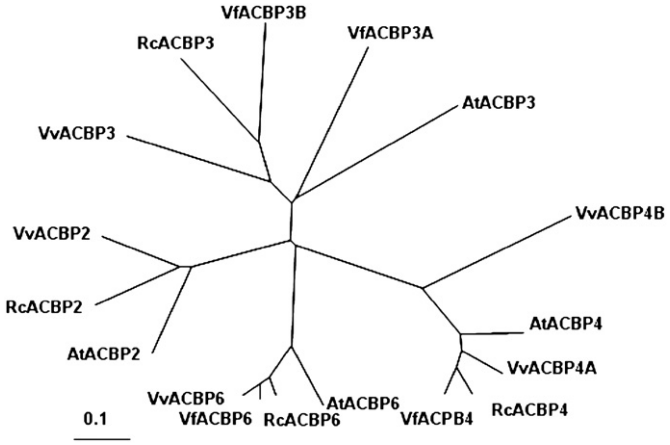

Fig. 2. Phylogenetic comparisons of Classes I–IV ACBPs from tung, castor bean, grape, and *Arabidopsis*. Class I proteins are designated ACBP6, Class II proteins are designated ACBP2, Class III proteins are designated ACBP3, and Class IV are designated ACBP4. The alignment was generated using ClustalX version 2.0.12 [42], and the resulting neighbor-joining tree is displayed graphically with TREEVIEW [46]. The branch lengths of the tree are proportional to divergence. The "0.1" scale represents 10% change.

compared in Fig. 3. *VfACBP3A* is expressed at higher levels in very young seeds, while both genes are expressed nearly equally during the remainder of seed development and in flowers. The most striking difference between the two profiles occurs in leaves, where *VfACBP3A* expression dominates. These results suggest at least partially redundant functions for the two tung ACBP3 proteins, except perhaps in young leaves. *Arabidopsis* ACBP3 participates in age-dependent and starvation-induced phospholipid turnover in leaves. Yet, like VfACB3A, AtACBP3 is also expressed at high levels in healthy, young rosette leaves [24], suggesting that these two proteins may share a conserved function unrelated to senescence [24] or pathogen defense [35,36]. The function of plant ACBP3s in seeds is also not yet clear, although a related role in phospholipid metabolism is likely, given the central role of acyl-CoA and PC in seed membrane lipid and TAG biosynthesis.

3.5. Transient transformation of cultured tobacco cells and immunofluorescence microscopy

All class III ACBPs described to date contain a putative transmembrane domain (TMD) very near their respective N-termini

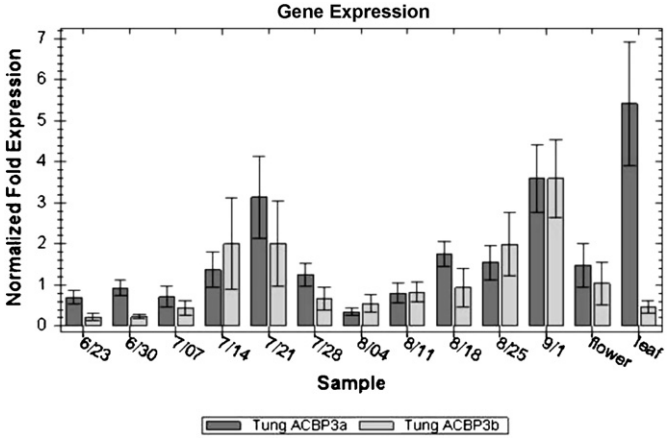

Fig. 3. Gene expression profiling of tung ACBP3A and ACBP3B. Total RNA was extracted from developing tung flowers and young expanding leaves harvested in April 2006, and from developing tung seeds at weekly intervals, from June 23 (6/23) through September 1 (9/1) of that year.

(Fig. 1**A**). The location of the TMD suggests that if may function as a signal-anchor sequence to help target these proteins to the plasma membrane *via* the secretory pathway. Once at the plasma membrane, the signal sequence might be cleaved, resulting in of the mature ACBP into the apoplast, or extracellular space. Initial investigations of subcellular targeting of C-terminally truncated AtACBP3 [23] suggested an apolastic destination; recent studies with the full-length protein confirmed apoplastic targeting, but also showed localization to the ER/Golgi complex, and intracellular membranes [24]. We performed detailed investigations of the subcellular targeting of full length AtACBP3, VfACBP3A, and VfACBP3B, each tagged with monomeric GFP (mGFP) at the C-terminus. mGFP was appended to the C-terminus of ACBP (with the stop codon removed during cloning) so as not to mask any effects on targeting by the N-terminal TMD, and also to be consistent with the AtACBP3-GFP fusion protein studied by Xiao et al. [24]. The ACBP-mGFP fusion proteins were introduced into tobacco BY-2 suspension cells by biolistic bombardment and then examined using epifluorescence microscopy. As shown in Fig. 4, all three plant ACBP3 fusion proteins displayed reticular immunofluorescence patterns similar to the staining pattern of endogenous ER labeled with fluor-conjugated concanavalin A (ConA). Notably, no plasma membrane or extracellular localization for any of the three ACBP3 proteins was detected. This result was also confirmed in transiently transformed and plasmolyzed onion epidermal cells (data not shown).

3.6. Recombinant His6-ACBP3 fusion protein expression and functional analysis

Previous studies of recombinant AtACBP3 showed that this protein preferentially binds polyunsaturated acyl-CoAs [23,24]. The rice class III protein, OsACBP5, has approximately equal affinity for palmitoyl-CoA (a saturated 16-carbon species) and linolenoyl-CoA (a trienoic 18-carbon acyl-CoA). N-terminal polyhistidine fusions of both tung ACBP3 proteins and AtACBP3, each containing an approximately equal portion of the central region N-terminal to the ACB domain through to their respective C-termini (Table 1), were produced in *E. coli*. All three proteins were detected in the soluble fraction after IPTG induction. The three recombinant ACBP3s were purified over nickel beads, to high purity (~80–95% pure) and yield (Fig. 5). All three fusion proteins migrate at anomalously high apparent molecular masses on SDS-PAGE. This observation is consistent with that of other plant ACBPs expressed in *E. coli* [12], and may be related to the high negative charge of these proteins at neutral pH (Table 1). All three proteins were assayed for binding to either oleoyl- or arachidonyl-CoA by Lipidex-1000 assays. Our AtACBP3 construct, unlike that used in previous studies [23,24] showed approximately 3-fold preference for monounsaturated oleoyl-CoA relative to polyunsaturated arachidonyl-CoA. Tung ACBP3A also preferred oleoyl-CoA, by a factor of approximately two. Tung ACBP3B showed very low binding to both acyl-CoAs tested (Fig. 6).

3.7. Three-dimensional modeling and structural predictions for ACBP3 proteins from tung and Arabidopsis

All plant ACBPs, including class III proteins, share the ancient conserved ACB domain four α-helix bundle structure [4,12,23]. Much less is known however, about the predicted secondary and tertiary structures of the other regions of the proteins. We investigated the predicted 3-D structures of the variable central regions and C-terminal ACB domains of *Arabidopsis* and tung ACBP3s. The full-length proteins were initially included to generate pdb files, but for sake of clarity, only those regions contained in the *E. coli*

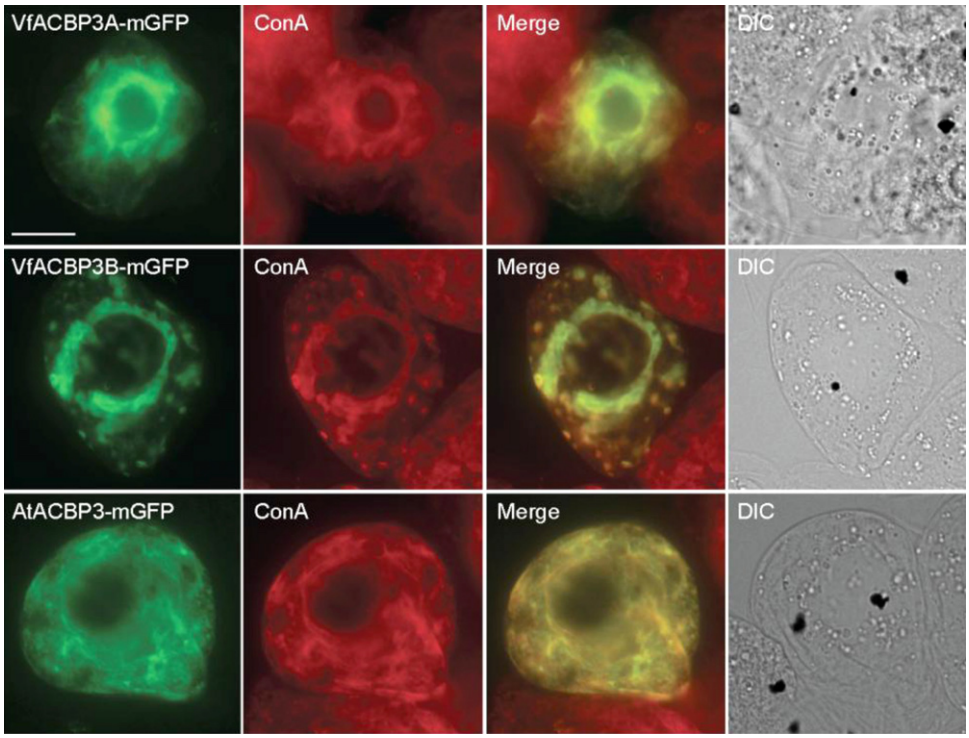

Fig. 4. Subcellular localization of tung and *Arabidopsis* ACBP3 proteins transiently expressed in tobacco BY-2 suspension cells. Shown are representative epifluorescence micrographs of BY-2 cells transiently transformed with plasmids encoding C-terminal mGFP-tagged tung ACBP3A (top row), ACBP3B (middle row), or *Arabidopsis* ACBP3 (bottom row). Cells were incubated with the ER stain ConA just prior to imaging. The corresponding merged and differential interference contrast (DIC) images of each cell are shown on the right. Bar = 10 μm.

expression constructs (Table 1) were included in the modeling predictions.

Solvent-excluded molecular surface images were rendered for each protein, in which the ribbon diagrams of the molecules were embedded. Folding of the secondary structures could be visualized in this mode of viewing. In all three proteins, the four α-helix bundle ACB domain is located in the C-terminal region of the molecule. For VfACBP3A, residues E106 through C-terminal residue A273 are visualized in Fig. 7**A**. The four α-helix bundle ACB domain starts with residue L170 and ends at S255. The N-terminal region of the truncated molecule shows 2 α-helices. A coil consisting of 32 amino acids links this region to the four α-helix bundle domain. No β-sheets were observed in this portion of VfACBP3A.

The region of VfACBP3B molecule from D150 to C-terminal E376 is shown in Fig. 7**B**. The N-terminus region of the visualized molecule had an abundance of α-helices. Altogether, there are 6 α-helices, four short and two long. Like VfACBP3A, β-sheets are noticeably absent in the entirety of the partial VfACBP3B molecule. The C-terminal extension present in VfACBP3B, which extends beyond the ACB, also contains 2 short α-helices and one long α-helix.

AtACBP3 (from Q162 to C-terminal P362) has a substantially different three-dimensional structure than the other two ACBP3s. The N-terminus of truncated AtACBP3 has 3 anti-parallel β-sheets, which is absent in both tung proteins (Fig. 7**C**). This portion of the protein has a short α-helix, followed by 3 β-sheets and 2 short α-helices, located just N-terminal to the ACB domain. The C-terminal end of the molecule has one long coil (from L316 through E343) which is followed by an α-helix.

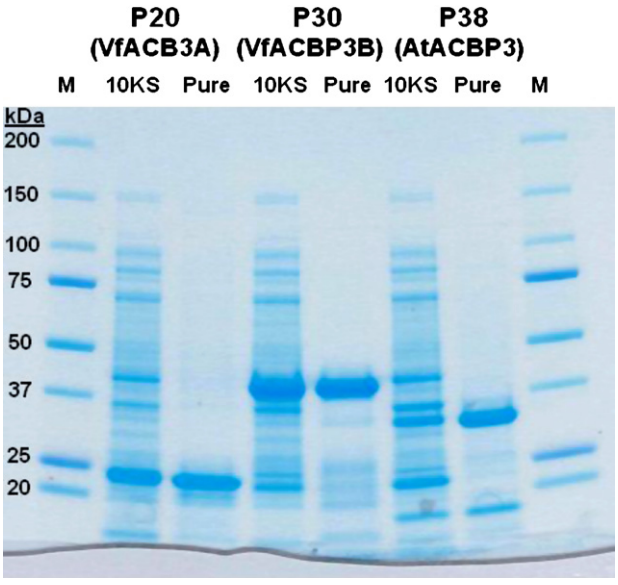

Fig. 5. SDS-PAGE analysis of semi-purified *E. coli*-expressed His6-ACBP3 fusion proteins. Partial ACBP3 proteins, fused at their N-termini to a polyhistidine tag were produced as described in Section 2. Cell pellets were lysed and particulate fractions removed by centrifugation at 10,000 × *g*. The 10 K supernatants were used as protein sources for Ni-NTA affinity purifications as described in Section 2. Fractions containing signficant amounts of target protein were pooled, dialyzed, and used in acyl-CoA binding assays. M, marker; 10KS, 10,000 × *g* supernatant; Pure, purified pooled protein.

4. Discussion

Our laboratories seek to understand the underlying molecular mechanisms that drive the efficient synthesis and accumulation of seed oils containing novel fatty acids, including α-eleostearic acid, an unusual trienoic fatty acid (18:3 $\Delta 9^{cis}$, 11^{trans}, 13^{trans}) that imparts industrially useful drying qualities to the oil from seeds of tung tree (*Vernicia fordii*) [37]. We have identified several

Table 1
E. coli expression vector information.

(N-terminal residues correspond to sequence from pET47b expression vector, first residue of plant ACBP3 protein marked in bold and underlined)

Clone:
VfACBP3A Glu106 N-His6
Sequence:
MAHHHHHHSAA**E**IEIVDLTEEGCEENSIDKSEIDMGLINEELGIYKDEMNCEIDGIKEGLLDDE
EDDWEGIERSELEKRFGAAVAYVGSIDNANKLSSTLSNGLKLQLYGLHQVAIEGPCHLPQPMPL
KFSARSKWNAWQQLGNMSPEMAMEQYINLVSTSIPEWMKDAFGDQVRKLHA
MW: 20.2 KDa
Apparent MW (estimated by SDS-PAGE): ~25 KDa
1 μg = 49.568 pmole
Isoelectric point: 4.63
Charge at pH 7: -19.42
Stock number: pP20

Clone:
VfACBP3B Asp150 N-His6
Sequence:
MAHHHHHHSAA**D**KSFTEKSEEVIEEKQKGEIESIGIEFAAEHDVVEESEEIRIVDSEAKEKAEE
KKIEIESDEDDWEGIERSELEQIFAKAAKFVESGDKDEGLTSVGSDVQMELYGLHKVATEGPCR
EQPPMALKVAARAKWNAWQRLGNMNPEVAMEQYVALVSDKVPGWMEDKSTDNGKPGSTEAANHG
ALPSDLSTSSSHHPYITEERNPEVAPGTEKNDLTGGLILENRATE
MW 26.2 kDa
Apparent MW ~42kDa
1 μg = 38.087 pmole
Isoelectric point: 4.67
Charge at pH 7: -27.19
Stock number: pP30

Clone:
AtACBP3 Gln162 N-His6
Sequence:
MAHHHHHHSAA**Q**EEVTELGRSGCVENEESGGDVLVAESEEVRVEKSSNMVEESDAEAENEEKTE
LTIEEDDDWEGIERSELEKAFAAAVNLLEESGKAEEIGAEAKMELFGLHKIATEGSCREAQPMA
VMISARAKWNAWQKLGNMSQEEAMEQYLALVSKEIPGLTKAGHTVGKMSEMETSVGLPPNSGSL
EDPTNLVTTGVDESSKNGIP
MW 23.0 kDa
Apparent MW ~32kDa
1 μg = 43.470 pmole
Isoelectric point: 4.46
Charge at pH 7: -28.46

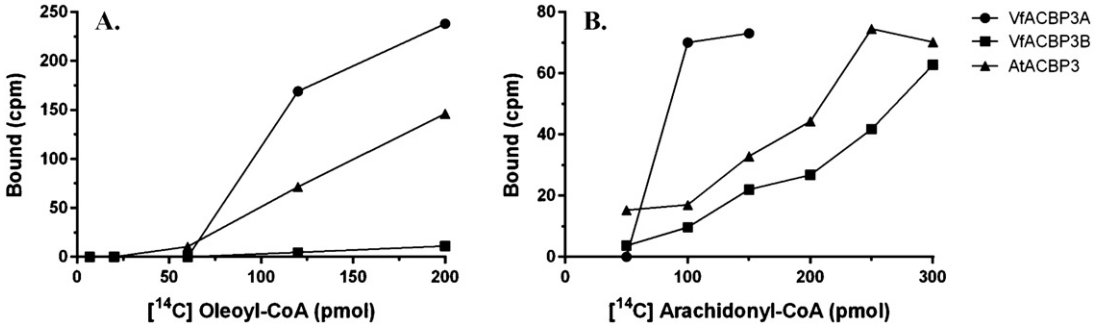

Fig. 6. Comparison of acyl-CoA binding properties by Lipidex-1000™ assays. Semi-purified His6-ACBP3 fusion proteins (see Table 1 and Fig. 5) were incubated with increasing concentrations of ^{14}C-labeled oleoyl-CoA or arachidonyl-CoA. Bound radioactivity was quantified as described in Section 2.

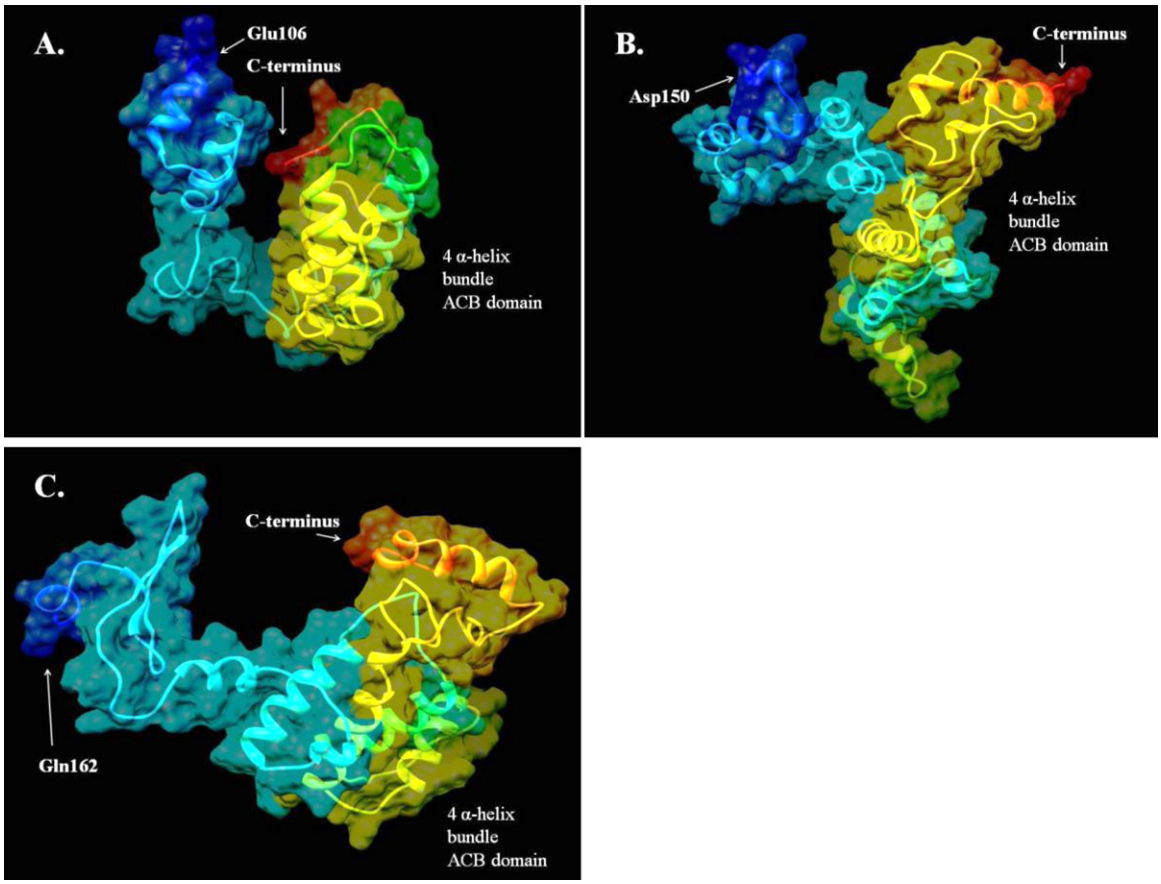

Fig. 7. Three-dimensional model predictions for N-terminal domains of VfACBP3A (panel A), VfACBP3B (panel B) and AtACBP3 (panel C). 3-D models were generated with Robetta. Molecular surface images, with embedded secondary structure ribbon diagrams, were generated using Deep-View and Chimera software programs. Color shading begins with dark blue at the N-termini, finishing with red at the C-termini. The respective N-terminal residues and C-termini are marked with arrows. The locations of the conserved four α-helix bundle ACB domains are also indicated.

important enzymes and co-factor proteins required for the production of fatty acid components in tung oil, including fatty acid desaturases (FAD) [38,39], fatty acid conjugase [25], glycerol-3-phosphate acyltransferases (GPAT) [40], diacylglycerol acyltransferases (DGAT) [27], cytochrome b5 (Cb5) [41], and Cb5 reductase [42]. However, efficient transgenic reconstitution of the entire tung oil biosynthetic pathway, or that of any other novel vegetable oil, will likely require inclusion of several enzymes and other regulatory and accessory proteins. Targeted searches for particular classes of tung lipid metabolic genes have been effective [27,41], but we also have expanded our gene discovery efforts to include anonymous searches for genes expressed during the middle to late stages of tung seed development, during which TAG biosynthesis is maximal [27]. Given the significant roles played by ACBP in yeast lipid metabolism, we searched these annotated tung seed cDNA sequence datasets for putative tung ACBP genes.

Multiple isoforms of *ACBP* genes are expressed in developing tung seeds. *VfACBP4* and *VfACBP6*, encoding predicted soluble ACBP proteins, were identified, as were two loosely related genes with modest amino acid identity to AtACBP3. Both *ACBP3*-like genes contained a well-conserved ACB domain located near their respective C-termini, a unique feature of class III ACBP proteins, thus these two genes were named *VfACBP3A* and *VfACBP3B*. Unlike the other three main classes of ACBP genes in higher plants, class III proteins are significantly more diverged (Fig. 2). The divergence between the two tung ACBP3 proteins can be seen in the C-terminal extension present in VfACB3B relative to VfACBP3A, the poor conservation of the central regions of the proteins, and multiple gaps and poor linearity of the central regions, leading to significantly different lengths of the full length proteins (Fig. 1**A**). The gene structures for *ACBP3* in tung are also only weakly similar, sharing only a conserved splice site at the 3′ end of the first exons. Otherwise, each gene has distinct exon/intron patterns (Fig. 1**B**), suggesting relatively ancient duplication of a common ancestral *ACBP3* gene. Castor bean, a closely related species in the Euphorbiaceae family, appears to have only one type III *ACBP* gene, which shares greater identity to tung ACBP3B (not shown). Most plant genomes studied to date also have only one *ACBP3*-type gene, although soybean may have at least four [12]. These results suggest that plant class III *ACBP* gene subfamilies have evolved and diversified much more than other types of *ACBP* genes, and that the relationship between speciation and *ACBP3* gene content and structure is very fluid. It is likely that class III ACBPs perform different functions in different species, and/or are able to achieve a common role despite the variability in the primary sequences.

Three-dimensional structure modeling and functional analysis through acyl-CoA binding assays also failed to unify the plant ACBP3 proteins in any obvious way. All three proteins share the ancient conserved 4 α-helix bundle ACB domain, which is the primary unifying component of the entire family of ACBP proteins [12]. However, each of the proteins likely adopts a significantly different folding pattern. The central region of VfACBP3A contains a long stretch of predicted random coil between the upstream α-helices and the C-terminal ACB domain (Fig. 7**A**). A narrow cleft is predicted between the central region and ACBP domain of this protein. VfACBP3B contains little predicted random coil in the central region, resulting in no cleft between the two domains (Fig. 7**B**). AtACBP3, on the other hand, is the only one of this set of class

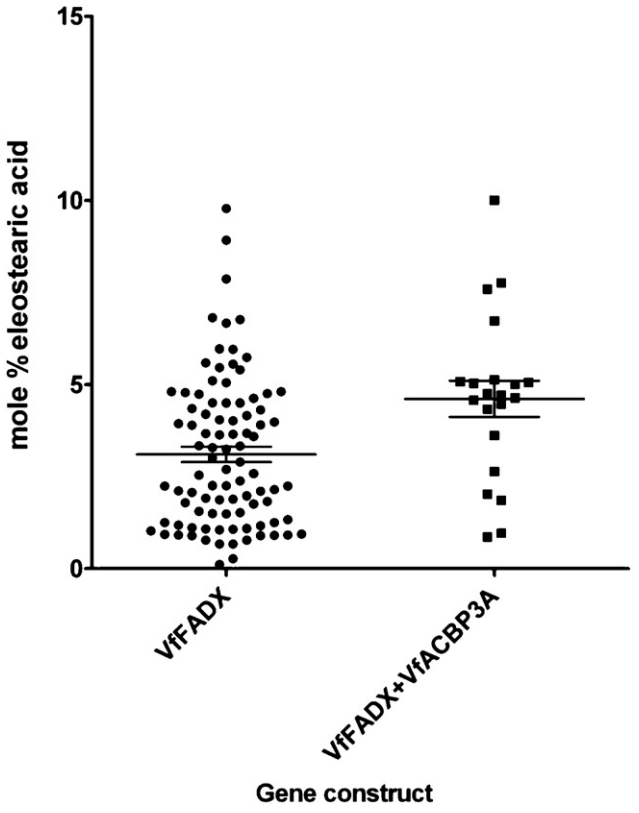

Fig. 8. Analysis of the eleostearic acid levels in seed lipids of transgenic Arabidopsis thaliana expressing tung proteins. Tung FADX, either alone or with tung ACBP3A, was expressed in seeds of *Arabidopsis thaliana*, as described in the text. Samples of segregating seed pools from T_1 transgenic plants were analyzed by gas chromatography. Each data point represents an independent transgenic event.

III ACBPs that contains predicted β-sheet structures in the central region, and the cleft between the two domains is much wider than that of VfACBP3A (Fig. 7**C**). These proteins were tested for binding to two acyl-CoA species, oleoyl-CoA (C18:1-CoA, a typical monounsaturated acyl-CoA species found in essentially all plant tissues) and arachidonyl-CoA (20:4-CoA, an unusually long and highly unsaturated acyl-CoA not commonly found in plant tissues). Arachidonyl-CoA was included in this analysis based on the results of previous studies that suggest a role for ACBP3 in biotic stress response, *via* disruption of pathogen signaling pathways, which often use arachidonate and related metabolites as signaling compounds [23,35,36]. Acyl-CoA binding assays revealed that both VfACBP3 proteins preferred oleoyl-CoA over arachidonyl-CoA, although the level of binding for VfACBP3B was very low with both substrates. Other saturated or polyunsaturated CoA esters common in tung tree tissues, such as palmitoyl-, linoleoyl-, linolenoyl-, or eleostearoyl-CoA may be better substrates for these proteins. Binding assays with these acyl-CoAs and phospholipids such as PC will be the focus of future experiments. AtACBP3 on the other hand, displayed different binding properties in our hands than those demonstrated previously [23,24]. These authors showed that AtACBP3 preferred polyunsaturated acyl-CoAs, with a significantly stronger affinity for arachidonyl-CoA than oleoyl-CoA. The opposite was observed in our studies (Fig. 6). The cause of the discrepancy is not clear. But it is perhaps noteworthy that our construct is longer, containing 54 additional residues N-terminal to the ACB domain, and our protein preparations were recovered from the soluble fraction of *E. coli*. Dr. Chye's studies used a shorter construct that was recovered from inclusion bodies by denaturation, followed by purification and renaturation. Given the differences in the predicted folding patterns of the proteins, it is possible that sequence upstream of the ACB influences the binding affinities of the respective ACBPs.

The results of subcellular targeting studies were also very intriguing. VfACBP3A, VfACBP3B, and AtACBP3 were all transiently expressed in tobacco BY-2 cells and found to distribute primarily to ER membranes (Fig. 4). In addition, ACBP3 proteins were occasionally detected in small, punctate locales distinct from many other known subcellular structures (data not shown). The identity of these structures is currently unknown. Future studies will be required to clarify whether the observed punctate structures are ACPB3-specific ER subdomains, similar to the subdomains observed previously for tung DGAT1, DGAT2 [27], GPAT8 and GPAT9 [37]. Plasma membrane and extracellular targeting was not observed in our case, despite compelling evidence for partial targeting of AtACBP3 to the plasma membrane and interstitial fluids of transgenic *Arabidopsis* plants overexpressing this gene [24]. More analysis will be necessary to attempt to reconcile these conflicting results, but the present data are consistent with the apparently complex subcellular distribution of ACBP3 proteins in plant cells [24].

AtACBP3 has a clear role in phospholipid metabolism, as it relates to age-dependent senescence [24]. What is not clear is the role of ACBP3 proteins in other plant organs and tissues. *AtACBP3* [24] and *VfACBP3A* (Fig. 4) are highly expressed in young leaves, a non-senescing tissue. *AtACBP3* is not strongly expressed in seeds, but both tung ACBP3 genes are expressed at relatively high levels throughout the middle to latter stages of tung seed development (Fig. 3), similar to rice *OsACBP5*, which is the only rice *ACBP* that is strongly expressed in this tissue [12]. Recent studies in both leaf and seed tissue [43,44] have shown that in many (probably most) plants, PC is a critical metabolite pool through which a majority of fatty acid flux and desaturation is controlled. Tung FADX also acts on fatty acids bound to PC to produce α-eleostearic acid [25]. It is possible that ACBP3s, containing both PC-binding and acyl-CoA binding properties, could be involved in PC-mediated membrane lipid biosynthesis and fatty acid remodeling. Co-expression of VfACBP3A with VfFADX in transgenic Arabidopsis lines revealed a small, but significant, increase in total seed eleostearic acid levels, compared to the levels produced by VfFADX alone (Fig. 8). These data support a potential, as yet unknown role, for tung ACBP3 proteins in PC metabolism as it relates to triacylglycerol biosynthesis. This possibility, along with the potential role of ACBP3s in plant defense against bacterial and/or fungal pathogens, makes ACBP3s an attractive target for additional future biotechnological studies.

Conflict of interest

The authors report no conflicts of interest that could inappropriately influence this work.

Acknowledgements

This work was supported by the United States Department of Agriculture, Agricultural Research Service (Current Research Information System project number 6435-41000-106-00D to K.S., A.H.J.U., CM., H.C., and J.S.), the Louisiana Board of Regents, Governor's Biotechnology Initiative (J.S. and S.P.), and the Natural Sciences and Engineering Research Council (S.G. and R.T.M.)

References

[1] A.C. Simonsen, U.B. Jensen, N.J. Færgeman, J. Knudsen, O.G. Mouritsena, Acyl-coenzyme A organizes laterally in membranes and is recognized specifically by acyl-coenzyme A binding protein, FEBS Lett. 552 (2003) 253–258.
[2] B. Gaigg, T.B. Neergaard, R. Schneiter, J.K. Hansen, N.J. Faergeman, N.A. Jensen, J.R. Andersen, J. Friis, R. Sandhoff, H.D. Schroder HD, J. Knudsen, Depletion of

acyl-coenzyme A-binding protein affects sphingolipid synthesis and causes vesicle accumulation and membrane defects in *Saccharomyces cerevisiae*, Mol. Biol. Cell 12 (2001) 1147–1160.
[3] N.J. Færgeman, S. Feddersen, J.K. Christiansen, M.K. Larsen, R. Schneiter, C. Ungermann, K. Mutenda, P. Roepstorff, J. Knudsen, Acyl-CoA-binding protein, Acb1p, is required for normal vacuole function and ceramide synthesis in *Saccharomyces cerevisiae*, Biochem. J. 380 (2004) 907–918.
[4] K.V. Andersen, F.M. Poulsen, Three-dimensional structure in solution of acyl-coenzyme A binding protein from bovine liver, J. Mol. Biol. 226 (1992) 1131–1141.
[5] B.B. Kragelund, K.V. Andersen, J.C. Madsen, J. Knudsen, F.M. Poulsen, Three-dimensional structure of the complex between acyl-coenzyme A binding protein and palmitoyl-coenzyme A, J. Mol. Biol. 230 (1993) 1260–1277.
[6] D.M. van Aalten, K.G. Milne, J.Y. Zou, G.J. Kleywegt, T. Bergfors, M.A. Ferguson, J. Knudsen, T.A. Jones TA, Binding site differences revealed by crystal structures of *Plasmodium falciparum* and bovine acyl-CoA binding protein, J. Mol. Biol. 309 (2001) 181–192.
[7] N.J. Færgeman, M. Wadum, S. Feddersen, M. Burton, B.B. Kragelund, J. Knudsen, Acyl-CoA binding proteins; structural and functional conservation over 2000 MYA, Mol. Cell. Biochem. 299 (2007) 55–65.
[8] O.P. Yurchenko, C.L. Nykiforuk, M.M. Moloney, U. Ståhl, A. Banas', S. Stymne, R.J. Weselake, A 10-kDa acyl-CoA-binding protein (ACBP) from *Brassica napus* enhances acyl exchange between acyl-CoA and phosphatidylcholine, Plant Biotechnol. J. 7 (2009) 602–610.
[9] C. Walz, P. Giavalisco, M. Schad, M. Juenger, J. Klose, J. Kehr, Proteomics of curcurbit phloem exudate reveals a network of defence proteins, Phytochemistry 65 (2004) 1795–1804.
[10] N. Suzui, S. Nakamura, T. Fujiwara, H. Hayashi, T. Yoneyama, A putative acyl-CoA-binding protein is a major phloem sap protein in rice (*Oryza sativa* L.), J. Exp. Bot. 57 (2006) 2571–2576.
[11] Q.F. Chen, S. Xiao, M.-L. Chye, Overexpression of the *Arabidopsis* 10-kilodalton acyl-CoA-binding protein ACBP6 enhances freezing tolerance, Plant Physiol. 148 (2008) 304–315.
[12] W. Meng, Y.C. Su, R.M. Saunders, M.L. Chye, The rice acyl-CoA-binding protein gene family: phylogeny, expression and functional analysis, New Phytol. 189 (2011) 1170–1184.
[13] M.-L. Chye, B.-Q. Huang, S.Y. Zee, Isolation of a gene encoding *Arabidopsis* membrane-associated acyl-CoA binding protein and immunolocalization of its gene product, Plant J. 18 (1999) 205–214.
[14] H.-Y. Li, M.-L. Chye, Membrane localization of *Arabidopsis* acyl-CoA binding protein ACBP2, Plant Mol. Biol. 51 (2003) 483–492.
[15] W. Gao, S. Xiao, H.-Y. Li, S.-W. Tsao, M.-L. Chye, Arabidopsis thaliana acyl-CoA-binding protein ACBP2 interacts with heavy-metal-binding farnesylated protein AtFP6, New Phytol. 181 (2009) 89–102.
[16] S. Xiao, W. Gao, Q.-F. Chen, S. Ramalingam, M.-L. Chye, Overexpression of membrane-associated acyl-CoA-binding protein ACBP1 enhances lead tolerance in *Arabidopsis*, Plant J. 54 (2008) 141–151.
[17] Q.-F. Chen, S. Xiao, W. Qi, G. Mishra, J. Ma, M. Wang, M.-L. Chye, The Arabidopsis *acbp1acbp2* double mutant lacking acyl-CoA-binding proteins ACBP1 and ACBP2 is embryo lethal, New Phytol. 186 (2010) 843–855.
[18] P.E. Johnson, S. Rawsthorne, M.J. Hills, Export of acyl chains from plastids isolated from embryos of *Brassica napus* (L.), Planta 215 (2002) 515–517.
[19] S. Xiao, H.-Y. Li, J.-P. Zhang, S.-W. Chan, M.-L. Chye, Arabidopsis acyl-CoA-binding proteins ACBP4 and ACBP5 are subcellularly localized to the cytosol and ACBP4 depletion affects membrane lipid composition, Plant Mol. Biol. 68 (2008) 571–583.
[20] H.-Y. Li, M.-L. Chye, Arabidopsis acyl-CoA-binding protein ACBP2 interacts with an ethylene responsive element-binding protein, AtEBP, via its ankyrin repeats, Plant Mol. Biol. 54 (2004) 233–243.
[21] W. Gao, H.-Y. Li, S. Xiao, M.-L. Chye, Acyl-CoA-binding protein 2 binds lysophospholipase 2 and lysoPC to promote tolerance to cadmium-induced oxidative stress in transgenic *Arabidopsis*, Plant J. 62 (2010) 989–1003.
[22] H.-Y. Li, S. Xiao, M.-L. Chye, Ethylene-pathogen-inducible *Arabidopsis* acyl-CoA binding protein 4 interacts with an ethylene-responsive element binding protein, J. Exp. Bot. 59 (2008) 3997–4006.
[23] K.C. Leung, H.Y. Li, S. Xiao, M.H. Tse, M.-L. Chye, Arabidopsis ACBP3 is an extracellularly targeted acyl-CoA-binding protein, Planta 223 (2006) 871–881.
[24] S. Xiao, W. Gao, Q.F. Chen, S.W. Chan, S.X. Zheng, J. Ma, M. Wang, R. Welti, M.-L. Chye, Overexpression of *Arabidopsis* acyl-CoA binding protein ACBP3 promotes starvation-induced and age-dependent leaf senescence, Plant Cell 22 (2010) 1463–1482.
[25] J.M. Dyer, D.C. Chapital, J.-C. Kuan, R.T. Mullen, C. Turner, T.A. McKeon, A.B. Pepperman, Molecular analysis of a bifunctional fatty acid conjugase/desaturase from tung. Implications for the evolution of plant fatty acid diversity, Plant Physiol. 130 (2002) 2027–2038.
[26] A.P. Weber, K.L. Weber, K. Carr, C. Wilkerson, J.B. Ohlrogge JB, Sampling the *Arabidopsis* transcriptome with massively parallel pyrosequencing, Plant Physiol. 144 (2007) 32–42.
[27] J.M. Shockey, S.K. Gidda, D.C. Chapital, J.C. Kuan, P.K. Dhanoa, J.M. Bland, S.J. Rothstein, R.T. Mullen, J.M. Dyer, Tung tree DGAT1 and DGAT2 have nonredundant functions in triacylglycerol biosynthesis and are localized to different subdomains of the endoplasmic reticulum, Plant Cell 18 (2006) 2294–2313.
[28] H. Cao, D.C. Chapital, J.M. Shockey, K.T. Klasson, Expression of tung tree diacylglycerol acyltransferase 1 in *E. coli*, BMC Biotechnol. 11 (2011) 73.
[29] M.J. Lingard, S.K. Gidda, S. Bingham, S.J. Rothstein, R.T. Mullen, R.N. Trelease, *Arabidopsis* PEROXIN11c-e, FISSION1b, and DYNAMIN-RELATED PROTEIN3A cooperate in cell cycle-associated replication of peroxisomes, Plant Cell 20 (2008) 1567–1585.
[30] D.E. Kim, D. Chivian, D. Baker, Protein structure prediction and analysis using the Robetta server, Nucleic Acids Res. 32 (2004) W526–W531.
[31] E.F. Pettersen, T.D. Goddard, C.C. Huang, G.S. Couch, D.M. Greenblatt, E.C. Meng, T.E. Ferrin, UCSF Chimera—a visualization system for exploratory research and analysis, J. Comput. Chem. 25 (2004) 1605–1612.
[32] R.N. Beachy, Z.L. Chen, R.B. Horsch, S.G. Rogers, N.J. Hoffmann, R.T. Fraley, Accumulation and assembly of soybean beta-conglycinin in seeds of transformed petunia plants, EMBO J. 4 (1985) 3047–3053.
[33] P. Guerche, C. Tire, F.G. De Sa, A. De Clercq, M. Van Montagu, E. Krebbers, Differential expression of the Arabidopsis 2S albumin genes and the effect of increasing gene family size, Plant Cell 2 (1990) 469–478.
[34] M.A. Smith, H. Moon, G. Chowrira, L. Kunst, Heterologous expression of a fatty acid hydroxylase gene in developing seeds of *Arabidopsis thaliana*, Planta 217 (2003) 507–516.
[35] S. Xiao, M.-L. Chye, Overexpression of *Arabidopsis* ACBP3 enhances NPR1-dependent plant resistance to *Pseudomonas syringae* pv tomato DC3000, Plant Physiol. 156 (2011) 2069–2081.
[36] S.-X. Zheng, S. Xiao, M.-L. Chye, The gene encoding *Arabidopsis* acyl-CoA-binding protein 3 is pathogen inducible and subject to circadian regulation, J. Exp. Bot. 63 (2012) 2985–3000.
[37] N.O.V. Sonntag, Composition and characteristics of individual fats and oils, in: D. Swern (Ed.), Bailey's Industrial Oil and Fat Products, vol. 1, John Wiley & Sons, New York, 1979, pp. 289–477.
[38] J.M. Dyer, D.C. Chapital, J.W. Kuan, R.T. Mullen, A.B. Pepperman, Metabolic engineering of *Saccharomyces cerevisiae* for production of novel lipid compounds, Appl. Microbiol. Biotechnol. 59 (2002) 224–230.
[39] J.M. Dyer, D.C. Chapital, J.-C.W. Kuan, H.S. Shepherd, F. Tang, A.B. Pepperman, Production of linolenic acid in yeast cells expressing an omega-3 desaturase from tung (*Aleurites fordii*), J. Am. Oil Chem. Soc. 81 (2004) 647–651.
[40] S.K. Gidda, J.M. Shockey, M. Falcone, P.K. Kim, S.J. Rothstein, D.W. Andrews, J.M. Dyer, R.T. Mullen, Hydrophobic-domain-dependent protein–protein interactions mediate the localization of GPAT enzymes to ER subdomains, Traffic 12 (2011) 452–472.
[41] Y.T. Hwang, S.M. Pelitire, M.P. Henderson, D.W. Andrews, J.M. Dyer, R.T. Mullen, Novel targeting signals mediate the sorting of different isoforms of the tail-anchored membrane protein cytochrome b_5 to either endoplasmic reticulum or mitochondria, Plant Cell 16 (2004) 3002–3019.
[42] J.M. Shockey, P.K. Dhanoa, T. Dupuy, D.C. Chapital, R.T. Mullen, J.M. Dyer, Cloning, functional analysis, and subcellular localization of two isoforms of NADH:cytochrome b_5 reductase from developing seeds of tung (*Vernicia fordii*), Plant Sci. 169 (2005) 375–385.
[43] P.D. Bates, J.B. Ohlrogge, M. Pollard M, Incorporation of newly synthesized fatty acids into cytosolic glycerolipids in pea leaves occurs via acyl editing, J. Biol. Chem. 282 (2007) 1206–1216.
[44] P.D. Bates, T.P. Durrett, J.B. Ohlrogge, M. Pollard M, Analysis of acyl fluxes through multiple pathways of triacylglycerol synthesis in developing soybean embryos, Plant Physiol. 150 (2009) 55–72.
[45] M.A. Larkin, G. Blackshields, N.P. Brown, R. Chenna, P.A. McGettigan, H. McWilliam, F. Valentin, I.M. Wallace, A. Wilm, R. Lopez, J.D. Thompson, T.J. Gibson, D.G. Higgins, Clustal W and Clustal X version 2.0, Bioinformatics 23 (2007) 2947–2948.
[46] R.D. Page, TreeView: an application to display phylogenetic trees on personal computers, Computational and Applied Biosciences 12 (1996) 357–358.